High-speed, two-photon scanning microscope

Ki Hean Kim, Christof Buehler, and Peter T. C. So

We have developed a high-speed two-photon microscope with submicrometer resolution in real time. The imaging speed improvement of this system is obtained by the use of a high-speed polygonal mirror scanner. The maximum achievable scanning rate is 40 μs/line, which is approximately 100 times faster than conventional scanning microscopes. High-resolution fluorescence images were recorded in real time by an intensified CCD camera. Using this instrument, we have resolved cellular architecture in three dimensions and have monitored the movements of protozoas. More important, photodamage to biological specimens during video-rate imaging can be minimized with two-photon excitation as compared with other one-photon modalities.

OCIS codes: 110.0180, 120.3890, 170.0110, 170.5810, 180.2520.

1. Introduction

Two-photon microscopy[1–4] is poised to become an important new tool for noninvasive biomedical diagnosis. Two-photon excitation is a fluorescence technique providing an important opportunity to assess tissue biochemistry and structures down to the depth of several hundred micrometers.[5,6] Although the clinical potentials of two-photon microscopy have been demonstrated, significant engineering challenges remain in terms of adapting this technology to the clinical setting. A major difficulty is the slow imaging speed of typical two-photon microscopes that have frame rates between 0.5 to 10 s. Based on endogenous chromophore fluorescence, the typical time required for high-resolution imaging (500 optical sections) of a 200-μm-thick skin tissue is approximately an hour.[6] This long imaging time is clearly impractical in the clinical setting. In addition, the slow data-acquisition rate also causes problems in image registration owing to the unavoidable motions of the subjects.

Two approaches have been taken to bring two-photon imaging speed to the video rate (approximately 30 frames/s). One technique is based on line scanning.[7,8] A line-scanning approach reduces image acquisition time by covering the image plane with a line instead of a point. The line focus is typically achieved with a cylindrical element in the excitation beam path. The resulting fluorescent line image is acquired with a spatially resolved detector such as a CCD camera. The main drawback associated with line scanning is the inevitable degradation of the image point-spread function, especially in the axial direction. A second approach,[9,10] which has been termed multiphoton multifocal microscopy, is analogous to Nipkow disk-based confocal systems. This approach is based on a custom-fabricated scan lens composed of a specially designed lenslet array that focuses the incident laser into multiple focus spots at the field aperture plane. The lenslet array is arranged similar to the traditional Nipkow design. Rotation of the scan lens causes the projected focal spots of the lenslet array to cover the field aperture plane uniformly. A CCD camera is used to register the spatial distribution of the resulted fluorescent spots and to integrate them into a coherent image. The ability to image multiple sample regions simultaneously reduces total data-acquisition time. Resolution degradation is less in the case of multiple focal-spot scanning compared with line scanning. Multiple focal-spot scanning also has the advantage of being extremely robust.

This report describes a third method optimized for high-speed, deep tissue imaging. This method, which uses a high-speed polygonal mirror, is based on raster scanning of a single diffraction-limited spot. This instrument was adapted from a very successful reflected light confocal microscope designed for deep tissue imaging.[11] Since fluorescence is generated

K. H. Kim (kimki@mit.edu), Ch. Buehler (christof.buehler@pharma.Novartis.com), and P. T. C. So (ptso@mit.edu) are with the Department of Mechanical Engineering, Massachusetts Institute of Technology, 77 Massachusetts Avenue, Cambridge, Massachusetts 02139.

Received 30 November 1998; revised manuscript received 16 June 1999.

0003-6935/99/06004-06$15.00/0

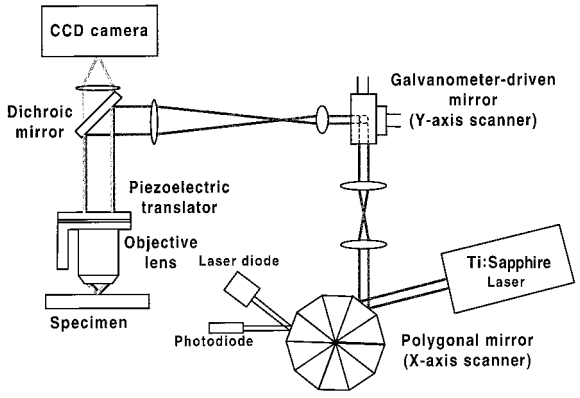

Fig. 1. Schematic of the high-speed, two-photon scanning microscope.

only at a single sample location at any given time, spatially resolved detection is not necessary. By replacing the CCD camera with a large, single-pixel detector such as a photomultiplier tube or an avalanche photodiode, one can also further improve the image resolution by removing the dependence on the emission point-spread function. The spatial information is encoded by the timing of the raster scan pattern as in typical confocal microscopy. This is particularly important in turbid specimens such as tissues in which the scattered fluorescence signal is not confined in a single pixel of the CCD camera and degrades the image resolution. The current setup of the system uses a CCD camera for the ease of implementation. In the future, a single-point detector will be implemented as a second channel in addition to the CCD camera to compare the two imaging modes in highly scattering specimens.

This report describes a new video-rate, two-photon scanning microscope design based on a high-speed polygonal mirror scanner. This system features diffraction-limited resolution and is optimized for deep tissue imaging. Preliminary results with this system include three-dimensional (3-D) cellular mitochondria distribution and the motion of protozoa. The advantages of two-photon scanning for noninvasive high-speed imaging are also discussed.

2. Experimental Method

The schematic of this video-rate two-photon microscopy design is presented in Fig. 1. A femtosecond Ti:Sapphire laser (Mira 900; Coherent, Palo Alto, California) is used to induce two-photon fluorescence. The microscope system is optimized for the excitation wavelength in the range of between 700 to 900 nm. The laser beam is rapidly raster scanned across a sample plane by means of two different scanners. A fast rotating polygonal mirror (Lincoln Laser, Phoenix, Arizona) accomplishes high-speed line scanning (x axis), and a slower galvanometer-driven scanner with 500-Hz bandwidth (Cambridge Technology, Watertown, Massachusetts) correspondingly deflects the line-scanning beam along the sample's y axis. The spinning disc of the polygonal mirror is composed of 50 aluminum-coated facets (2 mm $\times$ 2 mm) arranged contiguously around the perimeter of the disc. The facets repetitively deflect the laser beam over a specific angular range and correspondingly scan a line 50 times per revolution. Rotation speed of either 10,000, 15,000, 20,000 or 30,000 rpm can be selected. In the fastest mode, the corresponding scanning speed of 40 μs/line allows the acquisition of approximately one hundred 256 $\times$ 256 pixel images per second. The image acquisition rate is 100 times faster than conventional scanning systems.

Two lenses between the scanners function together as a relay element that projects the excitation beam deflected by the polygonal mirror onto a stationary point at the center of the y-axis scan mirror. The microscope is placed such that its telecentric plane intersects with the stationary point at the y-axis scan mirror. The laser beam is coupled into an upright microscope (Axioscope, Zeiss, Thornwood, New York) by means of a modified epiluminescence light path. The beam is reflected by the dichroic mirror toward the objective and is focused on the specimen. To perform 3-D volume scans, we mounted the objective on a computer-controlled piezoelectric objective translator with an approximate bandwidth of 300 Hz (P-721.00, Physik Instrumente, Waldbronn, Germany). The maximum z-axis travel range is 90 μm. The maximum push/pull capacity is 100/20 N. Its resolution is on the nanometer scale with feedback control. Translation of the objective axially yields z stacks of xy-plane images. The induced fluorescence signal is collected by the same objective and passes through the dichroic mirror. Residual scattered light is removed by an additional barrier filter (Schott BG39, Chroma Technology, Brattleboro, Vermont). The fluorescence is recorded by an intensified, frame-transfer CCD camera (Pentamax; Princeton Instrument, Trenton, New Jersey). The 12-bit data of the 512 $\times$ 512 pixel CCD chip can be read out at 5 MHz. The maximum achievable image transfer rate is approximately 11 frames/s for 256 $\times$ 256 pixel images (2 $\times$ 2 pixel binning). Currently, the CCD frame rate is the major obstacle in increasing frame speed of this system and can be improved by use of a faster imager. Consequently, the polygonal mirror's spinning speed is adjusted to 10,000 rpm, and the CCD exposure time is correspondingly set to 90 ms.

A separate laser diode (1 mW at 632 nm, Thorlab, Newton, New Jersey) along with a photodiode detector (Thorlab) is used to encode the polygonal mirror position and to generate a reference signal. This signal is used by a custom-built circuit board to synchronize the xy scanners, the objective translator, and the CCD camera (Fig. 2). The electronic circuit is based on reconfigurable logic (XS4010E, Xilinx, San Jose, California) that drastically enhances experimental flexibility.

For the given 76-MHz pulse repetition rate of the Ti:Sappire laser, only approximately 12 pulses hit the sample during a typical pixel dwell time of 0.16 μs. It is critical to optimize the light budget for both the excitation and the emission paths. Use of circular

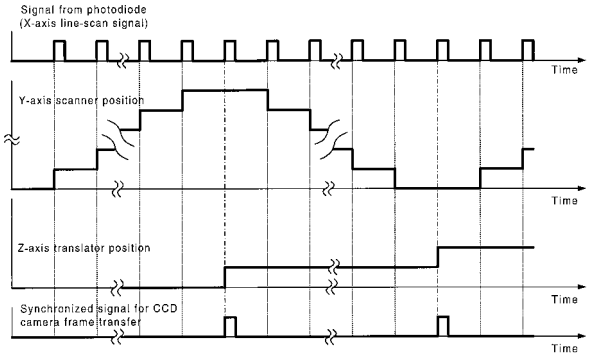

Fig. 2. Timing diagram for the synchronization of actuators and sensor. The signal from the photodiode is interpreted as an x-axis end-of-line signal. Y-axis scanner changes its position synchronously with this end-of-line signal. After 256 lines are scanned (one plane: 256×256 pixels), the z-axis piezoelectric objective translator steps to the next plane. CCD camera also runs synchronously with the piezoelectric translator.

instead of linear polarized laser light, allows the average excitation power to be increased by approximately 40% without excitation saturation of the sample, which is essential for maintaining the diffraction-limited excitation point-spread function. The linear-polarized light of the Ti:Sapphire laser is circularly polarized by a quarter-wave plate (CVI Laser Inc., Putnam, Connecticut). Next, both the deflection angle and the diameter of the scanning beam are balanced carefully to maximize the field of view and power throughput while still overfilling the objective's back aperture for diffraction-limited focusing. A number of objectives [Fluar 100×, numerical aperture (NA) 1.3, oil; Fluar 40×, NA 1.3, oil; Plan-Neofluar 25×, NA 0.8, water; Zeiss] were used in our experiments, and the corresponding line-scanning dimensions on the specimens are 45, 113, and 182 μm. Furthermore, these high-throughput objectives, along with a high-quantum-yield photodetector, allow us to acquire approximately 5% of the total emitted fluorescence. Assuming a typical two-photon excitation volume of 0.1 fl and a fluorophore concentration of 10 μM, approximately 70 photons per pixel can be acquired in the fastest scanning mode (25-kHz line rate), which is sufficient to generate useful images. Typically, for chromophore saturation to be avoided, the average laser power incident upon the sample surfaces was less than 10 mW, and the excitation wavelength was in the range of 730 to 780 nm.

3. Results and Discussions

To demonstrate real-time imaging with high spatial resolution, we stroboscopically recorded the piezo-driven linear displacement of a microscope slide that contained 2-μm-diameter, yellow-green latex spheres (Molecular Probes, Eugene, Oregon) immobilized in Fluoromount G (Southern Biotechnology, Birmingham, Alabama). The slide was attached to a computer-controlled piezostage that was mounted such that the spheres were shifted diagonally across the microscope's xy-image plane at a rate of 10 μm/s. An image series containing 100 frames was acquired at 780 nm. Three selected frames spanning equal amounts of time are depicted in Figs. 3(a)–3(c). If these motions were imaged at a slower rate, only the trajectories of these spheres could be seen, but the individual spheres would not be resolved. Figure 3(d) illustrates this point with a single image acquired by exposure of the sample to the CCD continuously for 9 s.

To demonstrate the potential of 3-D cellular imaging, we acquired a z-axis series of images of mouse fibroblast cells (CCL-92, ATCC, Manassas, Virginia) that had grown to approximately three cell layers thick on a cover-glass chamber slide (PGC, Gaithersburg, Maryland) containing 1 ml of medium. The sample was labeled with dihydrorhodamine (Molecular Probes), which is cell permeant and nonfluorescent. Dihydrorhodamine was first dissolved in dimethyl sulfoxide at a concentration of 10 mM. The stock probe solution was mixed with the medium in the chamber at a final concentration of 5 μM. With the presence of reactive-oxygen species within the cell, dihydrorhodamine was cleaved by reactive-oxygen species into individual fluorescent rhodamine molecules that localized in the mitochondria. One hundred images spanning a depth of 20 μm were acquired in 9 s with the excitation wavelength of 780 nm. The mitochondria distribution in the cell was visualized clearly in 3-D (Fig. 4). With successive scanning, the fluorescence intensity was observed to

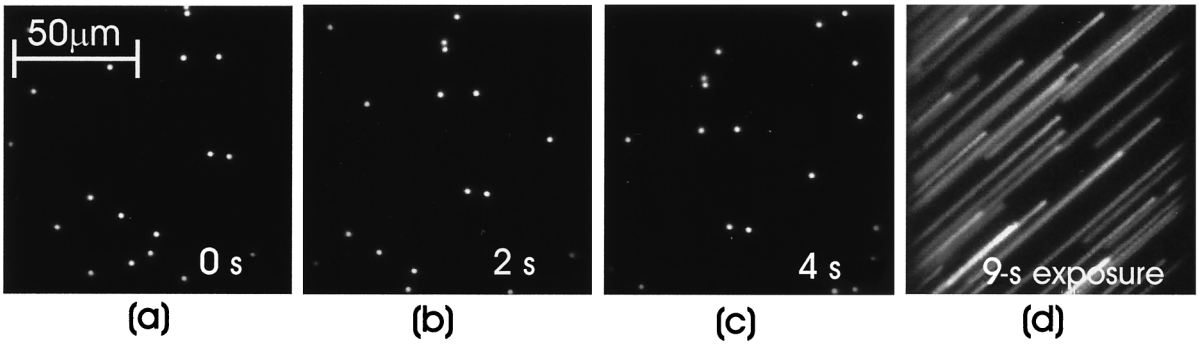

Fig. 3. (a)–(c) Time series of a 100-μm piezoinduced linear movement of 2-μm, yellow-green spheres. Three typical images of a movie of 100 frames are depicted. (d) Accumulative image over the same time course as in (a).

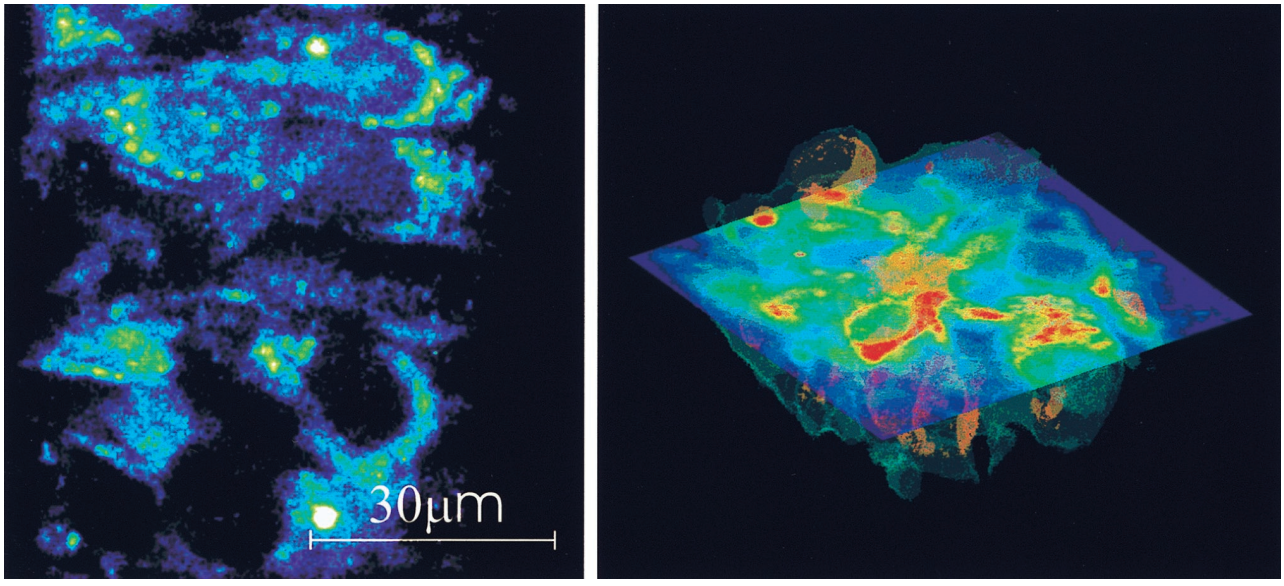

Fig. 4. Two-photon, 3-D resolved images of mitochondria distribution in mouse fibroblast cells as revealed with dihydrorhodamine labeling. Left panel shows a typical two-dimensional slice. Right panel shows the 3-D reconstruction.

increase consistently with photoinduced production of reactive-oxygen species in cells.

The characteristic movement of blepharisma, a protozoa species, was visualized in Fig. 5 (Fisher Scientific Co. Hampton, Vermont). The blepharisma sample was stained with 3 μM Calcein-AM (Molecular Probes) for 15 min. With the excitation wavelength of 780 nm, we acquired a time-lapse sequence of 100 images at the top surface of the coverslip. Images of the protozoas were captured as they swam across the scanning region. The characteristic expansion and contraction movement of the blepharisma was very fast; more than 50% change in the organism's body length could occur within 0.2 s. We could also track the rapid swimming motion of the organism at a rate as high as 1000 μm/s.

The reduction of photodamage is an important advantage of two-photon video-rate imaging as compared with traditional techniques, including wide-field fluorescence video microscopy and video-rate confocal

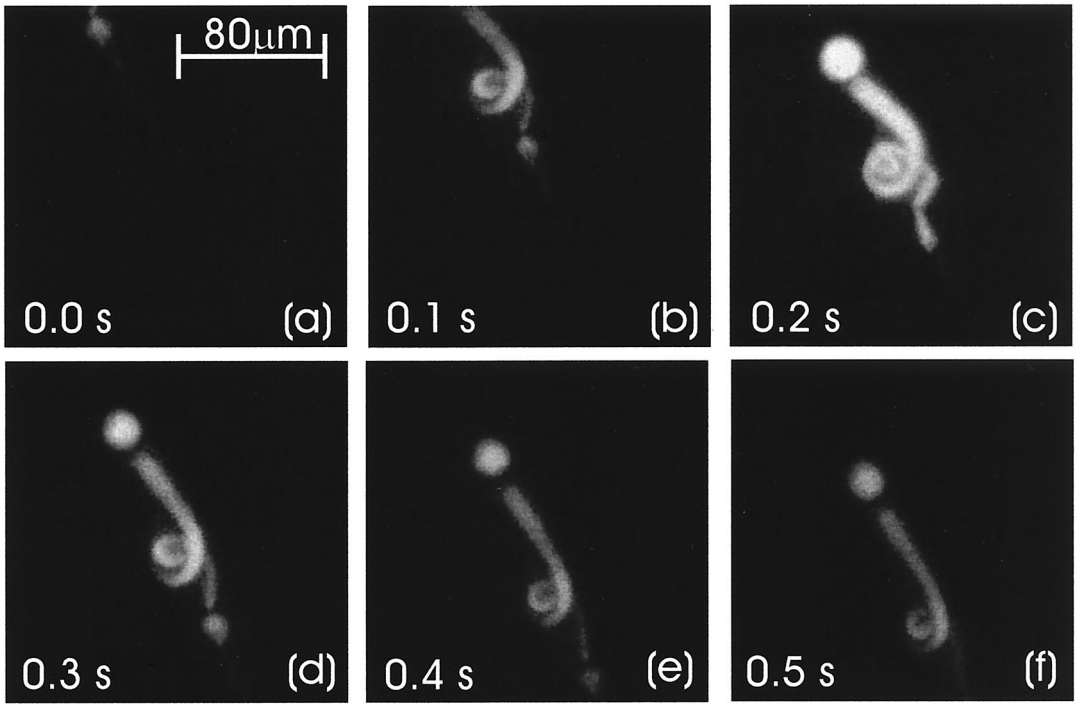

Fig. 5. Stroboscopically (11 frames/s) recorded movements of Calcein-AM-labeled blepharisma in an aqueous environment. Images were taken with the 25× water-immersion objective.

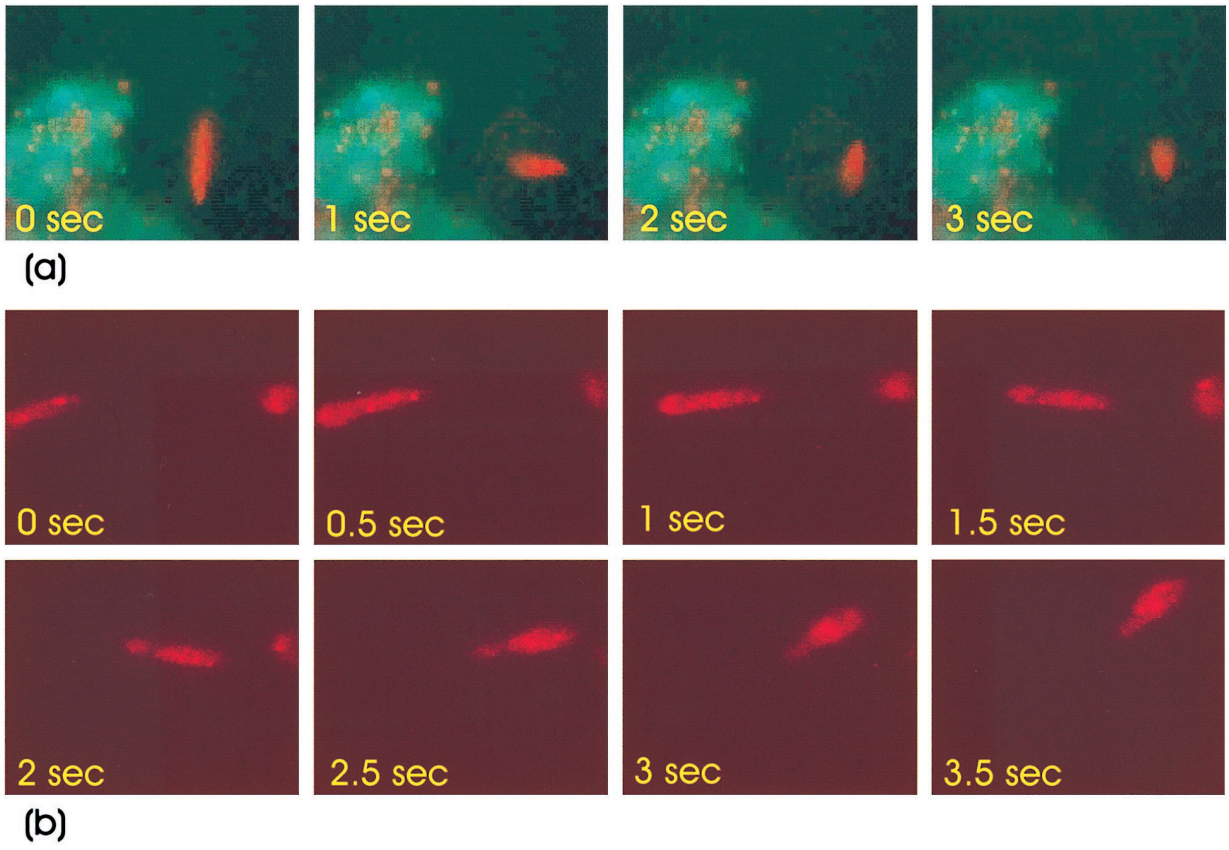

Fig. 6. Time-lapse sequences of euglena's movement. (a) Imaged with a wide-field fluorescence video microscope. Euglena was paralyzed within 3 s. (b) Imaged with a two-photon video-rate microscope. No photodamage was observed. The frame size is 62 μm.

microscopy. We used two-photon video-rate imaging with traditional wide-field fluorescence video microscopy to compare euglena locomotion. The imaging of euglena was based on their native chlorophyll fluorescence. A standard fluorescence microscope (Leitz, Orthoplan2, Stuttgart, Germany) equipped with a standard 100-W mercury arc lamp was used for wide-field fluorescence video microscopy. A three-color dichoric filter cube (Chroma Technology, Brattleboro, Vermont) simultaneously provided excitation wavelengths at 350, 480, and 510 nm. The fluorescence images were acquired by a video-rate 3-chip color camera (Sony, DXC-960MD). Time-lapse sequence images showing the response of a euglena to the arc-lamp excitation are shown in Fig. 6(a). With arc-lamp illumination, the euglena was observed to lose mobility almost instantly. The organism subsequently lost control of its cell shape within 3 s. The paralyzed euglena never regained activity after 10 s of data acquisition in a standard wide-field fluorescence microscope. In contrast, euglena motility could be noninvasively imaged by use of the two-photon video-rate microscope. A time-lapse sequence of euglena swimming across the imaging area is shown in Fig. 6(b). No loss of motility or cell shape control was ever observed for more than 30 euglenas that swam across the observation volume. Figure 6 demonstrates the less phototoxicity associated with two-photon video-rate imaging and the potential of this technology for future clinical application.

4. Conclusions

In conclusion, we have developed a high-speed, two-photon scanning microscope designed primarily for deep tissue imaging. We have obtained real-time tissue images with submicrometer resolution in three dimensions. We have shown that the main advantage of two-photon video-rate imaging lies with its low phototoxicity. The short, pixel dwell time due to high scanning speed requires us to optimize the light budget. Future improvement on the excitation efficiency may consist of compressing the laser pulses width by means of group velocity compensation and increasing the pulse repetition rate to approximately the inverse of typical fluorescence decay lifetimes. High-speed, 3-D, resolved two-photon microscopy provides new opportunities for the development of noninvasive biomedical applications, including optical biopsy, quantitative study of 3-D tissue architecture, and monitoring of wound healing and tissue regeneration.

References

1. W. Denk, J. H. Strickler, and W. W. Webb, "Two-photon laser scanning fluorescence microscopy," Science **248,** 73–76 (1990).

2. W. A. Mohler and J. G. White, "Stereo-4-D reconstruction and animation from living fluorescent specimens," Biotechniques **24,** 1006–1010 (1998).
3. B. D. Bennett, T. L. Jetton, G. Ying, M. A. Magnuson, and P. D. Piston, "Quantitative subcellular imaging of glucose metabolism within intact pancreatic islets," J. Biol. Chem. **271,** 3647–3651 (1996).
4. K. Svoboda, D. W. Tank, and W. Denk, "Direct measurement of coupling between dendritic spines and shafts," Science **272,** 716–719 (1996).
5. B. R. Masters, P. T. C. So, and E. Gratton, "Multi-photon excitation fluorescence microscopy and spectroscopy of in vivo human skin," Biophys. J. **72,** 2405–2412 (1997).
6. P. T. So, H. K. Kim, and I. E. Kochevar, "Two-photon deep tissue *ex vivo* imaging of mouse dermal and subcutaneous structures," Opt. Exp. **3,** 339–350 (1998).
7. G. J. Brakenhoff, J. Squier, T. Norris, A. C. Bliton, W. H. Wade, and B. Athey, "Real-time two-photon confocal microscopy using a femtosecond, amplified Ti:sapphire system," J. Microsc. **181,** 253–259 (1996).
8. J. B. Guild and W. W. Webb, "Line scanning microscopy with two-photon fluorescence excitation," Biophys. J. **68,** 290a. (1995).
9. J. Bewersdorf, R. Pick, and S. W. Hell, "Multifocal multiphoton microscopy," Opt. Lett. **23,** 655–657 (1998).
10. A. H. Buist, M. Muller, J. Squier, and G. J. Brakenhoff, "Real time two-photon absorption microscopy using multipoint excitation," J Microsc. **192,** 217–26 (1998).
11. M. Raijadhyaksha, M. Grossman, D. Esterowitz, R. H. Webb, and R. R. Anderson, "*In vivo* confocal scanning laser microscopy of human skin: melanin provides strong contrast," J. Investigative Dermatol. **6,** 946–952 (1995).